Journal of Nuclear Materials 468 (2016) 56–70

Contents lists available at ScienceDirect

Journal of Nuclear Materials

journal homepage: www.elsevier.com/locate/jnucmat

Modeling of sink-induced irradiation growth of single-crystal and polycrystal zirconiums in nuclear reactors

Sang Il Choi [a], Gyeong-Geun Lee [b], Junhyun Kwon [b], Ji Hyun Kim [a, *]

[a] School of Mechanical and Nuclear Engineering, Ulsan National Institute of Science and Technology, 100 Banyeon-ri, Eonyang-eup, Ulju-gun, Ulsan 689-798, Republic of Korea
[b] Nuclear Materials Research Division, Korea Atomic Energy Research Institute, 1045 Daedeok-daero, Yuseong-gu, Daejeon 305-353, Republic of Korea

ARTICLE INFO

Article history:
Received 22 April 2015
Received in revised form
3 October 2015
Accepted 8 November 2015
Available online 14 November 2015

Keywords:
Irradiation growth
Irradiation sink
Mean-field rate theory
Irradiation growth strain
Grain boundary
Polycrystal and cold-worked zirconium

ABSTRACT

The objective of this study is irradiation growth modeling of polycrystal zirconium using the advanced mean-field rate theory (MFRT) and growth equation. Since the 1960s, irradiation growth of zirconium has been among the most important phenomena in nuclear reactors. However, there is no general irradiation growth model that can explain changes in both the microstructure morphology and growth strain in polycrystal zirconium owing to lack of knowledge of the relevant atomistic information and MFRT. Although two groups have developed a single-crystal zirconium irradiation growth model, a general polycrystal zirconium model has not been developed. In this study, therefore, the defect flux was calculated using the MFRT, and the dislocation loop density was calculated from the defect flux. Moreover, the bias factor for each sink (dislocation lines, loops, and grain boundaries) was adopted in the MFRT. In addition, dislocation line and grain boundary effects were examined in polycrystal zirconiums. Finally, irradiation growth equation was established and growth strain was calculated using the average strain factor and anisotropy factor considering grain-interaction. For single-crystal zirconium and cold-worked polycrystal zirconium, irradiation growth strain results show good agreement with the experimental results. For annealed polycrystal zirconium, the results deviate from the experimental results.

1. Introduction

Zirconium and its alloys are widely used as nuclear fuel cladding and guide tubes in commercial and research reactors because of their excellent radiation and corrosion resistance. However, despite these excellent properties, irradiation growth occurs. Irradiation growth is volume-conservative distortion without applied stress. It is distinguished from other radiation-induced dimensional changes such as swelling and creep. Radiation-induced swelling is isotropic volume expansion without any applied stress, whereas radiation-enhanced creep is volume-conservative distortion due to applied stress. Zirconium, hafnium, and titanium are representative materials that exhibit irradiation growth. Therefore, the in-pile behavior of zirconium has to be verified; hence, zirconium alloys have been demonstrated by many theoretical and experimental methods since the 1960s.

Traditionally, radiation-induced phenomenon such as swelling, creep, and growth are simulated using the mean-field rate theory (MFRT). The defect concentration and sink strength and density are calculated using the MFRT. In the early 1980s, much theoretical research on irradiation growth was based on the MFRT [1–3]. However, in early studies of the MFRT, this application was limited to the region of low displacements per atom (dpa) because of limited computation performance. Moreover, the MFRT could not possibly explain changes in the irradiation growth rate with temperature because there was no fundamental understanding of irradiation phenomenon. Therefore, irradiation growth modeling failed to precisely predict zirconium irradiation growth. However, at the end of the 1980s, these problems were solved by the development of two concepts. First, Woo suggested the diffusion anisotropy difference (DAD) concept, which explains that irradiation growth is caused by the difference between the diffusion coefficients of the <*a*> and <*c*> axes [4,5]. Second, Holt et al. [6] showed that the production bias model (PBM) effects this difference. The PBM concept, which is based on computer simulation science, assumes different fractions of interstitial and vacancy

* Corresponding author.
E-mail address: kimjh@unist.ac.kr (J.H. Kim).

http://dx.doi.org/10.1016/j.jnucmat.2015.11.014
0022-3115/

clusters. In addition, with the development of computers, the calculation region for irradiation growth could be expanded to hundreds of dpa [7].

With progress in the MFRT, irradiation growth was calculated independently for single crystals by two groups, Christien et al. [8] and Golubov et al. [7]. Both of the calculation results show good agreement with measured single-crystal irradiation growth. Christien et al. used the cluster dynamics model (CDM) of point defects to calculate the growth. In this model, it was assumed that only point defects are mobile, and all the clustering defects are immobile. Although neutron-induced defects are not the only point defects, electron irradiation generates only point defects. Therefore, this model is quite reasonable for electron irradiation. However, Christien work has some argument in the modeling assumption. First, the diffusion coefficient used in their model was much smaller (10^{-1} order) than the computer-simulated value [9]. Second, the defect concentration was assumed to be homogenous in the matrix; hence, the interstitial defect flux is much higher than the vacancy defect flux anywhere. Therefore, only an interstitial dislocation loop could survive in the prism plane in the framework. In contrast, Golubov et al. [7] used the PBM to calculate the growth strain. The concept of the PBM is opposite to that of the CDM. Specifically, interstitial clusters are mobile defects in the PBM but not in the CDM. Therefore, in the PBM framework, interstitial clusters could be the most important influence on the growth modeling result. However, Golubov et al. [7] neglected the effect of defect recombination. Therefore, the work of both groups has certain limitations. The irradiation growth rate of cold-worked polycrystal zirconium was calculated in a wide temperature range [6]. However, this model did not explain the irradiation growth of annealed polycrystal and single-crystal zirconium because dislocation line, loop, and grain boundary effects are harder to predict than those of cold-worked polycrystal zirconium.

Therefore, there is no general prediction model of irradiation growth that could explain zirconium from single crystals to polycrystals, although prediction modeling of single-crystal zirconium growth and cold-worked polycrystal zirconium has been done using the MFRT and growth equation. Therefore, this paper focuses on theoretical modeling of single-crystal and annealed and cold-worked polycrystal zirconium irradiation growth, which could fully explain the microstructure and growth strain. To predict the growth of various types of zirconium, a simplified assumption was developed that point defects evolve directly from sinks such as dislocation loops, dislocation lines, and grain boundaries.

2. Methodology

2.1. Irradiation growth mechanisms

To model irradiation growth of zirconium, several basic mechanisms should be defined. First, the sink characteristics are simply defined by the results of experimental work because the characteristics of sinks have been identified as the most fundamental reason for irradiation growth of zirconium by an experiment at Northern Research Laboratories of United Kingdom Atomic Energy Authority [10–15]. Next, the effects of sinks on irradiation growth of zirconium are established by considering the sink characteristics. Finally, in order to describe polycrystal irradiation growth, the effect of grain interaction was briefly reviewed.

2.1.1. Characteristics of sinks

In single-crystal zirconium, unlike the polycrystal case, grain boundaries are not considered [10,11]. Therefore, dislocation lines and loops are the major sinks causing irradiation growth. Dislocation loops are either <*a*> or <*c*> dislocation loops, which are perpendicular to the corresponding axis. Experimental results have confirmed that all <*a*> and <*c*> dislocation loops have a uniform direction [16–19]. Specifically, <*a*> dislocation loops have a Burgers vector $\vec{b} = 1/3 <1\,1\,2\,0>$, which is parallel to the *a* axis and lies in the prismatic plane $(10\bar{1}0)$. Moreover, these types of loops are observed to coexist as vacancy and interstitial types in the prism plane. In contrast, <*c*> dislocation loops lie in the (0 0 0 1) plane, and the Burgers vector is $\vec{b} = 1/2 <0\,0\,0\,1>$ or $\vec{b} = 1/6 <2\,0\,\bar{2}\,3>$ along the *c* axis [20]. Further, <*a*> dislocation loops are generated immediately after irradiation, whereas <*c*> dislocation loops appear after several dpa.

In polycrystal zirconium, dislocation loops and lines are generally considered to be main sinks, and grain boundaries are also considered to be main sinks [12–15]. However, the sink characteristics of grain boundaries are hard to establish experimentally owing to their three-dimensional shapes. Therefore, several different models of the sink strength of grain boundaries are considered in the MFRT. (Physically, the sink strength determines the defect reaction rate with the sink at a given defect diffusivity and concentration.) Among these models, that derived by Brailsford and Bullough [21] considers the sink strength of grain boundaries when the dislocation density is sufficiently high compared with that of any other sink. (This is explained further in section 3.1.) MacEwen and Carpenter [2] used Brailsford and Bullough's grain boundary model [21] because it was assumed that both annealed and cold-worked polycrystal zirconium have a high number of dislocation loops and high line density. However, MacEwen and Carpenter calculated irradiation growth of zirconium only at the beginning of the few-dpa region, and their results are inconsistent with experimental results owing to the lack of information in the experimental database and lack of atomistic constants. Therefore, Brailsford and Bullough's sink model of grain boundaries [21] is used in this model with the advanced MFRT and the latest constant. The sinks in hexagonal close-packed (hcp) zirconium are shown schematically in Fig. 1. The shapes and locations of dislocation loops, dislocation lines, and a grain boundary are sketched.

2.1.2. Effect of sinks on irradiation growth of zirconium

In dislocation line and loop-induced irradiation growth, defect reactions with dislocation lines and loops are the driving force. In the first stage, an irradiation defect is developed by the <*a*> dislocation lines and loops because they are interstitial bias sinks, as interstitials diffuse more rapidly than vacancies. This phenomenon could be expressed as a defect flux given by a diffusion coefficient ($D_{v\ or\ i}$) and a defect concentration ($C_{v\ or\ i}$). This concept is derived from the defect accumulation rate. Because the reaction rate with sinks is proportional to a given defect sink density, the defect flux is the defect accumulation rate at unit sink density. This concept is well established in the Brailsford and Bullough's work [21]; i.e., $D_iC_i >> D_vC_v$, where $D_i >> D_v$, and $C_v = C_i$ in dislocation lines and loops. Therefore, irradiation growth occurs in the <*a*> direction because <*a*> dislocation lines and loops have a Burgers vector of $\vec{b} = 1/3 <1\,1\,2\,0>$. In a single crystal zirconium, this initiation of irradiation growth, which is caused by the dislocation loop growth, occurrs in 0 ~ 1 dpa regime.

Next, in the middle stage, the <*a*> dislocation and loop densities are saturated because many of the interstitial defects are consumed by <*a*> dislocation loops. In this situation, <*c*> dislocation loops could be formed on the basal plane because the vacancy concentration is increasing; i.e., $D_iC_i = D_vC_v$, where $D_i >> D_v$, *and* $C_v >> C_i$. Because of the saturation of <a> dislocation loop in this stage, the strain of irradiation growth could be negligible in 1 ~ 4 dpa regime.

In the last stage, the <*c*> dislocation loops have consumed the vacancy defects in the basal plane. Therefore, the <*a*> dislocation lines and loops could absorb the interstitial defects, and the

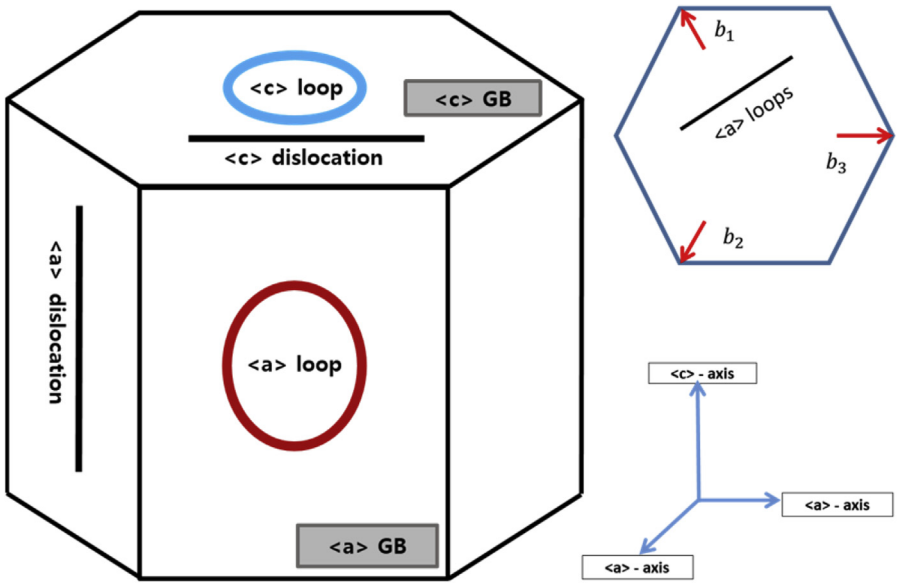

Fig. 1. Schematic of main sinks in zirconium.

vacancy defects are consumed by the <*c*> dislocation loops. Finally, irradiation growth is accelerated by the existence of both <*a*> and <*c*> dislocation lines and loops. However, the dislocation loop density is large enough that dislocation lines can be neglected; hence, it was assumed that the density of dislocation lines is not changed by the defect flux. This reaccelerated regime, where the growth is restarted at ~4 dpa, in irradiation growth is also called as a breakaway phenomenon.

In grain-boundary-induced irradiation growth, deformation occurs by the same mechanism as deformation by dislocation loops. The face of the grain boundary that is parallel to the prism plane induces <*a*>-axis elongation because the interstitial defect flux is dominant and the side. The face that is parallel to the basal plane induces <*c*>-axis shortening because of the vacancy defect flux. Like dislocation lines, grain boundaries are assumed to remain constant in size regardless of the defect flux because they are too large to be changed by the defect flux.

2.1.3. *Effect of grain interaction on the irradiation growth of zirconium*

The major difference between single crystal and polycrystal zirconium is the grain interaction caused by the distribution of each grain with different orientation in polycrystal. Each grain is constrained and deformed by neighbor grain, and this phenomena could make the irradiation growth more or less than when the grain interaction is not considered. In order to analyze the effect of grain interaction on growth, various experimental studies have been performed by Woo, Causey, Holt, and Adams [22–25]. It was conformed that the irradiation growth shows much complex behavior depending on mechanical properties of material and the condition of heat treatment. Not only texture but also residual stress is important parameter in an annealed polycrystal zirconium because the defect produced under irradiation is used for the relaxation of residual stress. In this study, it is assumed that annealed polycrystal was full relaxed, but the effect of residual stress could be negligible in case of cold work polycrystal because most of irradiation defect is consumed by dislocation loops.

2.2. *Mean-field rate theory*

The physical meaning of irradiation growth is bias rearrangement of atoms by reaction with irradiation defects and sinks. This reaction changes the atom number and morphology in the sink and eventually induces irradiation growth. Therefore, the MFRT uses a diffusion-limited reaction to calculate the defect flux and sink strength. Then, from the MFRT, the irradiation growth is calculated by the dislocation climb mechanism.

Specifically, the defect flux is described by the diffusion coefficient and defect concentration. The diffusion coefficient can be calculated more easily than the defect concentration experimentally and by computer simulation [9,26,27]. However, it is difficult to analyze the defect concentration experimentally because of the limitations of experimental tools.

Therefore, the defect concentration was calculated by the MFRT [28,29]. In this paper, the MFRT follows a recent method that includes dislocation loop development. The equation describing the increasing density of dislocation loops follows the scenario of Barashev et al. [30]. Moreover, to simplify the model, the cluster effect was replaced by sink development caused by point defect absorption. In single-crystal zirconium, dislocation loops and lines are the main sinks in the matrix. Therefore, the MFRT is simply expressed as

$$\frac{dC_{sv}}{dt} = K_o - K_{iv}C_{si}C_{sv} - \rho_{ilp}Z^v_{ilp}C_{sv}D_v - \rho_{vlb}Z^v_{vlb}C_{sv}D_v - \rho_{dp}Z^v_{dp}C_{sv}D_v - \rho_{db}Z^v_{db}C_{sv}D_v \quad (1)$$

$$\frac{dC_{si}}{dt} = K_o - K_{iv}C_{si}C_{sv} - \rho_{ilp}Z^i_{ilp}C_{si}D_i - \rho_{vlb}Z^v_{vlb}C_{si}D_i - \rho_{dp}Z^i_{dp}C_{si}D_i - \rho_{db}Z^i_{db}C_{si}D_i \quad (2)$$

where $C_{sv\ or\ si}$ is interstitial or vacancy concentration (cm^{-3}) of single-crystal zirconium, K_0 is the defect generation rate ($cm^{-3}s^{-1}$) which mean vacancy and SIA are combine and go to perfect lattice atom. K_{iv} is recombination rate (cm^3s^{-1}), ρ_{ilp} is density of interstitial loop, which lay in prism plane (cm^{-2}), ρ_{vlb} is density of vacancy loop in basal plane (cm^{-2}). ρ_{dp} is density of dislocation line, which parallel with prism plane, ρ_{dp} density of dislocation line, which parallel with basal plane (cm^{-2}), Z^i_{ilp} is interstitial bias factor of interstitial

loop in prism plane, Z^{v}_{ilp} is vacancy bias factor of interstitial loop in prism plane, Z^{i}_{vlb} is interstitial bias factor of vacancy loop in basal plane, Z^{v}_{vlb} is vacancy bias factor of vacancy loop in basal plane, Z^{i}_{dp} is interstitial bias factor of dislocation line, parallel with prism plane, Z^{v}_{dp} is vacancy bias factor of dislocation line, parallel with prism plane, Z^{i}_{db} is interstitial bias factor of dislocation line, parallel with basal plane, Z^{v}_{db} is vacancy bias factor of dislocation line, parallel with basal plane, $D_{v\ or\ i}$ diffusion coefficient of vacancy or interstitial in the matrix ($cm^2 s^{-1}$). The effect of the bias factor will be explained in next section. The follow detail constant in next section are given in Table 1.

The first term on the right-hand side of Eq. (1) is the defect generation rate; the second is the recombination rate; the third is the vacancy absorption rate of <a> interstitial loops, which are parallel to the prism plane; the fourth is the vacancy absorption rate of <c> vacancy loops, which are parallel to the basal plane; the fifth is the vacancy absorption rate of <a> dislocation lines, which are perpendicular to the prism plane; the last is the vacancy absorption rate of <c> dislocation lines, which are perpendicular to the basal plane. The MFRT of vacancies follow the same method as that of interstitials. The effect of the bias factor will be explained in the section 3.2. The constants are listed in Table 1.

In polycrystal zirconium, dislocation loops and lines should be considered as the main sinks in the matrix, but grain boundaries also have to be added in the MFRT. Therefore, the MFRT of polycrystal zirconium is simply expressed using the single-crystal MFRT:

$$\frac{dC_{pv}}{dt} = \frac{dC_{sv}}{dt} - k^2_{gp} Z^{v}_{gp} C_v D_v - k^2_{gp} Z^{v}_{gp} C_v D_v \tag{3}$$

$$\frac{dC_{pi}}{dt} = \frac{dC_{si}}{dt} - k^2_{gp} Z^{i}_{gp} C_i D_i - k^2_{gb} Z^{i}_{gb} C_i D_i \tag{4}$$

where $C_{pv\ or\ pi}$ is defect concentration of vacancy and interstitial in polycrystal matrix (cm^{-3}), k^2_{gp} is sink strength of grain boundary, which is parallel with prism plane, k^2_{gb} is sink strength of grain boundary, which is parallel with basal plane, Z^{i}_{gp} is interstitial bias factor of grain boundary, which is parallel with prism plane, Z^{v}_{gp} is vacancy bias factor of grain boundary, which is parallel with prism plane, Z^{i}_{gb} is interstitial bias factor of grain boundary in basal plane, Z^{v}_{gb} is vacancy bias factor of grain boundary in basal plane.

Specifically, the first and second terms on the right-hand side of Eqs. (3) and (4) are the vacancy absorption rates of <a> and <c> grain boundaries, respectively. In the polycrystal equation, the sink strength of the grain boundary was calculated using Brailsford and Bullough's method. The constants are listed in Table 1.

In the MFRT, it is assumed that the dislocation line density does not change because dislocation loops absorb all the defect flux. In contrast, the dislocation loop density is a defect-flux-dependent variable. The total density of dislocation loops and lines can be calculated as

$$\rho_{total} = \rho_{dp} + \rho_{db} + 2\pi r_v N_v + 2\pi r_i N_i \tag{5}$$

where r_v and r_i are the dislocation loop radii of vacancies and interstitials (cm), and N_v and N_i are the dislocation loop number densities of vacancies or interstitials (cm^{-3}), respectively. The loop number density is hard to calculate by a theoretical method because there is no general equation for loop nucleation and growth equation under radiation. Therefore, the experimental value of the loop number density was used. However, the dislocation loop radius could be calculated by a theoretical equation [30].

As described in Eqs (1) and (2), vacancy dislocation loops in prismatic plane are not considered in this study because the consideration of co-existence of vacancy and interstitial is needed to modify the fundamental assumption of MFRT. Since MFRT assumes that all sink is homogenously distributed and these sink receive same defect flux, the expression of co-existence of vacancy and interstitial dislocation loops are neglected in this study. However, since the reaction probability was calculated by MFRT using average defect flux value of each sink, vacancy loops in prismatic plane could be neglected without having any problem in the situation where the sinks are distributed homogeneously.

2.3. Irradiation growth strain model

The rate of irradiation growth strain is determined not only by

Table 1
Input parameters.

Input parameter		Symbol	Unit	Value	Reference/comment
Defect generation rate		G	$s^{-1}\ cm^{-3}$	10^{-7}	[42]
Recombination radius		r_{iv}	cm	10^{-7}	[8]
Burgers vector		b	cm	3.23×10^{-8}	[43]
Diffusion coefficient	Vacancy	D_v	$cm^2\ s^{-1}$	3.0×10^{-17}	[8]
	SIA	D_i	$cm^2\ s^{-1}$	1.0×10^{-6}	[8]
Sink strength	<a> loop	ρ_{ilp}	cm^{-2}	$2\pi r_i N_i$	[7]
	<c> loop	ρ_{vlb}	cm^{-2}	$2\pi r_v N_v$	[7]
	<a> dislocation line	ρ_{dp}	cm^{-2}	Single: 7.25×10^6	[35]
				Cold: 20×10^9	[35]
	<c> dislocation line	ρ_{db}	cm^{-2}	Single: 2.25×10^6	[35]
				Cold: 5×10^9	[35]
	<a> GB	$(k_{GB}/2)$	cm^{-2}	$6 \times \sqrt{\rho} \div d_{gb}$	[21]
	<c> GB	$(k_{GB}/2)$	cm^{-2}	$6 \times \sqrt{\rho} \div d_{gb}$	[21]
Average strain factor	<a> loop	A_{ilp}	Constant	0.5	[31]
	<c> loop	A_{vlb}	Constant	1.0	[31]
	<a> dislocation line	A_{dp}	Constant	0.5	[31]
	<c> dislocation line	A_{db}	Constant	1.0	[31]
	<a> GB	A_{GBp}	Constant	0.5	Assumed in this work
	<c> GB	A_{GBp}	constant	0.5	Assumed in this work
Bias factor	<a> loop	Z^{i}_{ilp}	Constant	1	[44]
	<c> loop	Z^{i}_{vlb}	Constant	0.586	[4]
	<a> dislocation line	Z^{i}_{dp}	Constant	1.56	[4]
	<c> dislocation line	Z^{i}_{db}	Constant	0.586	[4]
	<a> GB	Z^{i}_{gp}	Constant	1.56	[4]
	<c> GB	Z^{v}_{gb}	Constant	0.586	[4]

defect reactions with sinks but also by the average strain. The concept of the average strain as a factor was first suggested by Dollins. Before this concept was suggested, irradiation growth was assumed to directly reflect the dislocation line and loop size. However, in Dollins's work, dislocation loops and lines induce dimensional changes in any given direction, which are analyzed using a schematic figure. From this quantitative analysis, irradiation growth by dislocation lines and loops could be expressed in terms of an average strain value. Therefore, the average strain factor effect was considered in the irradiation growth equation for single-crystals. For polycrystals, the effect of texture (the anisotropy of each grain direction) is also considered in the model. In addition to this development, the growth strain rate is calculated for each sink type. For single crystals, irradiation growth is simply expressed in terms of the dislocation loop density and defect flux because *a*-axis elongation and *c*-axis shortening are caused directly by dislocation loops. An anisotropy factor was not considered because grains do not exist in single crystals. The irradiation growth strain rate was calculated using the dislocation climb mechanism. The general rate of strain and dislocation climb velocity can be described by the simple equations

$$\frac{d\varepsilon}{dt} = \rho b V \tag{6}$$

$$V = \frac{1}{b}\left(Z_i D_i C_i - Z_v D_v C_v\right) \tag{7}$$

where ε is the elongation (cm), ρ is the dislocation density (cm^{-2}), b is the Burgers vector (cm), v is the dislocation velocity ($cm^{-2}s^{-1}$), and z_i and z_v are the interstitial and vacancy bias factors of dislocations, respectively.

Physically, Eq. (6) expresses all the dimensional changes that could explain the creep- and stress-induced strain. These phenomena occur along one direction. However, irradiation growth occurs along various directions because the defect flux originates in neutron bombardment. Therefore, this general equation is limited to the calculation of each sink strain. Because of the anisotropy of the interstitial diffusion coefficient, the defect flux is specified for each sink. (For vacancies, the diffusion coefficient is always isotropic because the activation energy is much higher than that of interstitials.) From these equations, irradiation growth could be calculated for a specific sink type.

The bias factor is also considered to affect the capture efficiency because it determines the reaction probability of defect and sink reactions. In an hcp system, the bias factor depends on the DAD because the crystal structure is anisotropic [4,5]. Therefore, the detailed irradiation growth equation of a single crystal is expressed for each sink type:

$$\frac{d\varepsilon_a^{ilp}}{dt} = A_{ilp}\rho_{ilp}\left(Z_{ilp}^{i} D_i C_i - Z_{ilp}^{v} D_v C_v\right) \tag{8}$$

$$\frac{d\varepsilon_a^{dp}}{dt} = A_{dp}\rho_{dp}\left(Z_{dp}^{i} D_i C_i - Z_{dp}^{v} D_v C_v\right) \tag{9}$$

$$\frac{d\varepsilon_c^{vlb}}{dt} = A_{vlb}\rho_{vlb}\left(Z_{vlb}^{v} D_v C_v - Z_{vlb}^{i} D_i C_i\right) \tag{10}$$

$$\frac{d\varepsilon_c^{db}}{dt} = A_{db}\rho_{db}\left(Z_{db}^{i} D_i C_i - Z_{db}^{v} D_v C_v\right) \tag{11}$$

$$\frac{d\varepsilon_a}{dt} = \frac{d\varepsilon_{ilp}}{dt} + \frac{d\varepsilon_{dp}}{dt} \tag{12}$$

$$\frac{d\varepsilon_c}{dt} = \frac{d\varepsilon_{vlb}}{dt} + \frac{d\varepsilon_{db}}{dt} \tag{13}$$

where ε_a^{ilp}, ε_a^{dp}, ε_a^{vlb}, and ε_a^{db} are the irradiation growth strain induced by interstitial dislocation loops in the prism plane, dislocation lines parallel to the prism plane, vacancy dislocation loops in the basal plane, and dislocation lines parallel to the basal plane, respectively, and A_{ilp}, A_{dp}, A_{vlb}, and A_{db} are the corresponding average strain factors for each sink. The physical meaning of average strain factor is the average of effective strain in any give direction caused by sink growth or creation in a single crystal. In case of <a> dislocation loop, strain, which is calculated in any given direction in single crystal, is a function of cosine with angle. This, average of effectiveness of strain concept in any give direction was well described in Dollins's work [31]. Therefore, the average stain factor does not mean that the defect flux are changed, but, the degree of deformation is changed by the direction of sink in any given direction of hexagonal structure. The average strain factors for dislocation lines and loops are calculated according to the description of the average growth strain in the <*a*>- and <*c*>-axis directions for a certain direction. For <*a*> dislocation loops and lines, which are perpendicular to the <*c*> axis, the strain factor is 0.5, whereas for <*c*> dislocation loops and lines, which are parallel to the <*c*> axis, that is 1 [2,8,31]. ε_a and ε_c are the total radiation growth strain along the <*a*> and <*c*> axes, respectively. Finally, the calculation result of ε_a is compared with experiment results in Fig. 5.

In the growth equation for polycrystal zirconium, the grain boundary sinks and grain orientation (texture) are considered. Therefore, irradiation growth of polycrystal zirconium is expressed differently from that of single crystals. The average strain factor of grain boundaries is also considered after the <*a*>- and <*c*>-axis growth strain rate is calculated to determine the growth in a certain direction. The average strain factor of grain boundaries is 0.5 because an isotropic grain boundary distribution is assumed for sufficiently high annealing. Therefore, the growth strain rate equations including the texture are expressed as

$$\frac{d\varepsilon_a^{gp}}{dt} = A_{gp}k_{gp}^2\left(Z_{gp}^{i} D_i C_i - Z_{gp}^{v} D_v C_v\right) \tag{14}$$

$$\frac{d\varepsilon_d}{dt} = G_{poly} \times \left(\frac{d\varepsilon_a^{ilp}}{dt} + \frac{d\varepsilon_a^{dp}}{dt} + \frac{d\varepsilon_a^{gp}}{dt}\right) \tag{15}$$

where ε_d is irradiation growth strain in the direction of interest of polycrystal; and ε_a^{gp} are the irradiation growth strain induced by grain boundaries in the prism of single grain; A_{gp} are the average strain factors for grain boundaries in the prism of single grain; In order to calculate ε_d, anisotropy factor (G_{poly}) was induced in this Eq (15) because texture show anisotropic behavior in hexagonal structure. From anisotropy factor, the relationship between radiation growth of single crystal and polycrystal could be defined. In tradition, anisotropy factor was simply calculated by F factor (G_{poly}=1–3F) [13,32–34]. (The F factor is the resolved fraction of the basal poles in any given direction hence it give texture information by pole figure.) The anisotropy factor without considering grain-interaction is based on the assumption that the irradiation growth could be simply calculated by averaging in radiation growth of each grain which is distributed in various direction. However, recent studies reported that irradiation growth of polycrystal could

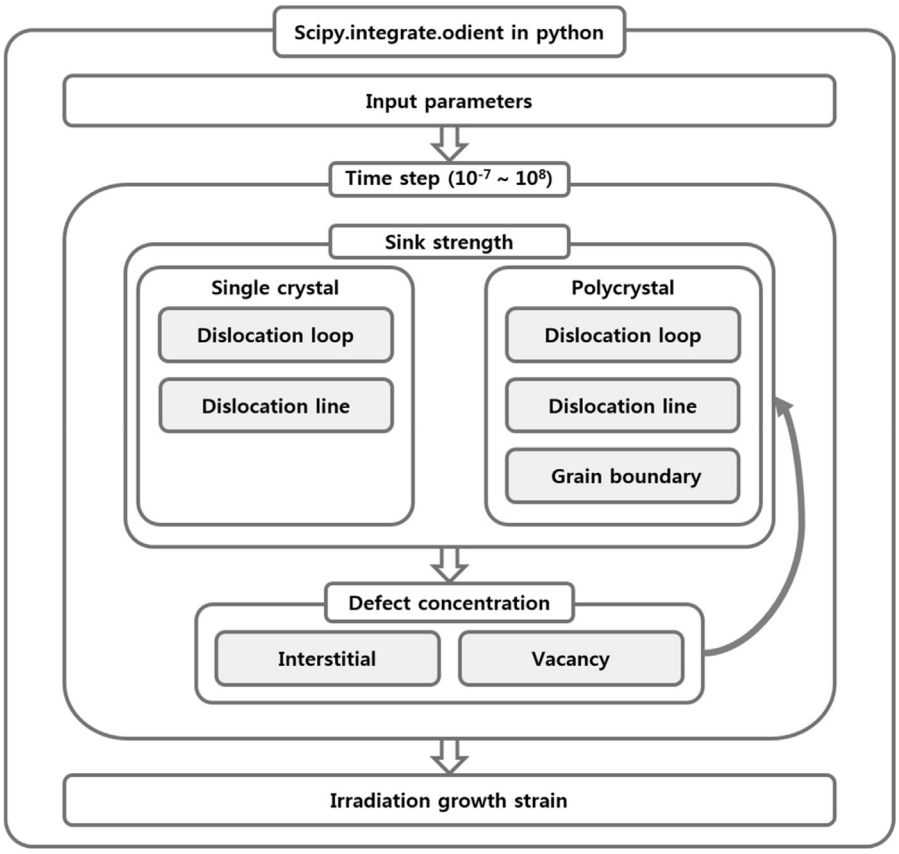

Fig. 2. Schematic diagram of model of irradiation growth of zirconium.

not be simply calculated by traditional method because the difference of each grain orientation induced the grain-interaction, as a consequence, the irradiation creep which could make irradiation growth more or less depending upon specimen directions [22–25]. Therefore, anisotropy factor, G_{poly}, considering the grain-interaction is defined as the relationship between single crystal and polycrystal irradiation growth in the direction of interest, which can be calculated by considering F factor and grain interaction at the same time.

2.4. Computer code implementation

Irradiation growth is assumed to occur by sink development. Specially, irradiation growth of single-crystal zirconium is induced by dislocation loops, which are the main sink in single crystals. Therefore, the dislocation loop density is first calculated using Eq. (5). An experimental result for the number density of dislocation loops is given in the Python code [17,18]. However, the dislocation loop radius is calculated using the defect flux. To calculate the defect flux, the defect concentration is calculated using Eqs. (1) and (2) in the MFRT, and then the defect flux is derived using the diffusion coefficient. Ultimately, from this information, the change in the dislocation loop density is calculated, and then the defect concentration is evaluated using the dislocation density calculated in each time step. It was assumed that <*c*> dislocation loops do not exist before 3 dpa because of the interstitial defect flux. Therefore, after 3 dpa, the <*c*> dislocation loop density is calculated by the same method as for <*a*> dislocation loops.

In polycrystal zirconium, grain boundaries are also a major factor in irradiation growth. Therefore, the sink strength of grain boundaries is calculated like that of dislocation loops by Brailsford and Bullough's model in the scipy.integrate.odeint system. The grain boundary sink strength is calculated using the density of dislocation loops and lines, and then the dislocation loops are evaluated. The dislocation line density is assumed to be independent of the defect flux. However, the initial dislocation line density is important input data in the Python code. Therefore, the value of the dislocation line density is obtained from an experimental result [35]. A schematic diagram of the sequence in polycrystal zirconium in this study is shown in Fig. 2.

3. Results & discussion

The irradiation growth strain is calculated by the MFRT and general dislocation climb equation. The results for both single-crystal and polycrystal zirconium are examined in terms of the defect concentration, defect flux, sink strength, and growth strain. The effect of dislocation lines and loops on growth was verified for single-crystal zirconium. The effect of grain boundaries on growth was confirmed for polycrystal zirconium. For annealed polycrystals, the grain boundary effect was an important parameter for dislocation lines and loops. In contrast, the grain boundary effect was negligible for cold-worked polycrystal zirconium. Finally, for verification, the calculation results are compared with experimental data.

3.1. Single-crystal zirconium

The defect concentration shows typical low-sink-density behavior in single-crystal zirconium [36]. Initially, the defect concentrations increases because reaction probability is too low to recombine or interact with sinks. Next, the interstitial defect

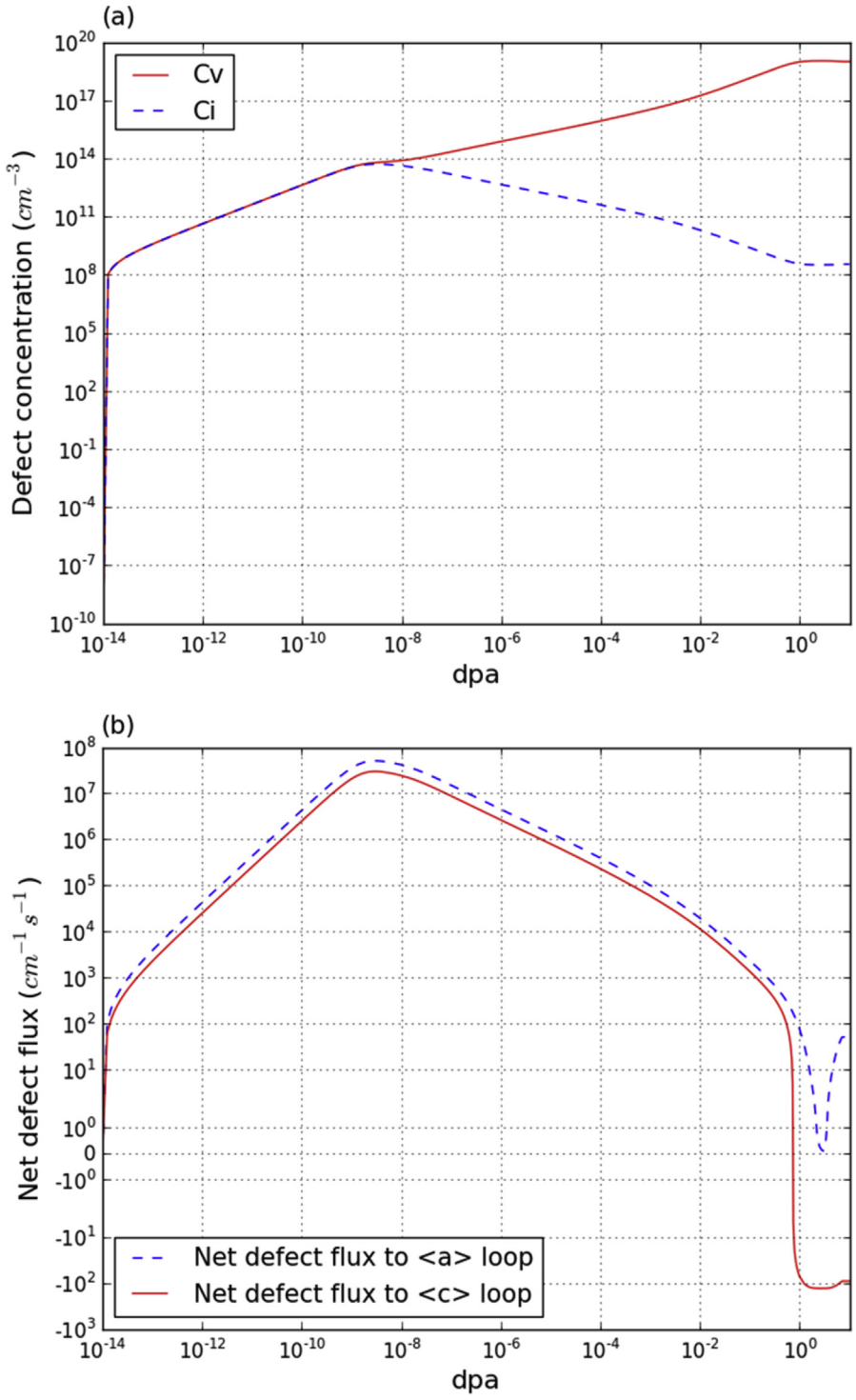

Fig. 3. Radiation-induced (a) point defect concentrations, and (b) net defect flux to dislocation loops in single-crystal zirconium at 553 K.

concentration decreases and the vacancy concentration increases because of rapid interstitial diffusivity. From this region, the defect react with sink, and the sink density is changed. Finally, point defects are in a steady state because the production rate could be compensated by the recombination rate (10^{-8}–1 dpa). Fig. 3 (a) shows the defect concentration of single-crystal zirconium.

From the calculated defect concentration, the interstitial net defect fluxes to the major sinks are calculated. In single-crystal zirconium, these are the <*a*> and <*c*> dislocation loops. Fig. 3 (b) shows the interstitial net defect flux to the sinks. The defect flux initially increases at 10^{-9} dpa and immediately afterward decreases up to 1 dpa. In this early stage, net defect flux occurs during a very short time. Therefore, sinks are not developed greatly, and the effect of this regained defect flux on irradiation growth is negligible. Therefore, the growth is actually affected in the steady-state net flux region, i.e., the high-dpa region. Finally, the net defect flux to <*a*> dislocation loops is positive, whereas the vacancy is negative because of the DAD, indicating that interstitial defects are

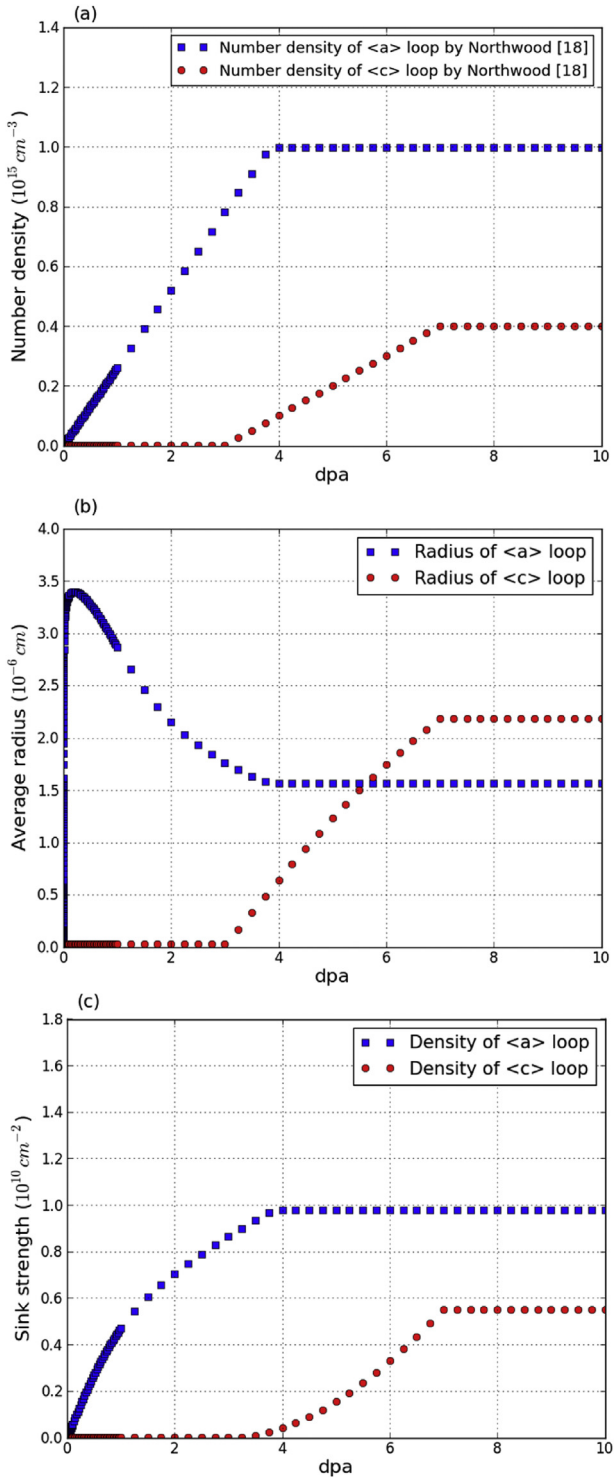

Fig. 4. Sink information of (a) number density, (b) average radius, and (c) sink strength in single-crystal zirconium at 553 K.

accumulated in <a> dislocation loops, and vacancies react with <c> dislocation loops. In this irradiation growth model, two types of dislocation loops are examined and calculated. The method of calculating the dislocation density follows that of Barashev et al. [30]. The number density of dislocation loops and the dislocation radius are used to calculate the dislocation density. Fig. 4(a) shows the number density of dislocation loops. The value of the former is obtained from an experimental database [17,18] and the radius is calculated using the change rate of the total number of defects:

$$\dot{S}_v = 2\pi r_v N_v (D_v C_{sv} - D_i C_{si}) \tag{16}$$

$$r_v = \sqrt{(S_v/\pi b N_v)} \tag{17}$$

where S_v is the total number of vacancies in the vacancy dislocation loops. The change in S_v could be calculated from the defect flux because the reaction probability is proportional to the circumference of the dislocation loops and the defect flux. The radius of interstitial dislocation loops can be calculated using the same equation as that used for vacancies. Fig. 4(b) shows the radius of the dislocation loops. For interstitial <a> loops, the radius increases dramatically in the early dpa region. Subsequently, the radius is in the steady state. For <c> dislocation loops, the radius increases linearly from 3 to 7 dpa. However, there is no general information about the number density of <c> dislocation loops. Much of the early-stage research presented only the ratio of the number densities of interstitial and vacancy loops [20,37]. Fortunately, the presence of <c> dislocation loops was analyzed by Holt and Gilbert [38,39] in order to understand breakaway phenomena. In zircaloy-2, <c> dislocation loops do not appear before the 3 dpa region.

Fig. 4 (c) shows the change in the dislocation loop density versus the dpa. Initially, the <a> dislocation loop density increases dramatically, whereas that of <c> type loops increases above <3> dpa. Next, the density of both types of dislocation loops shows a saturation region. The <a> dislocation loops are generated by the net interstitial defect flux behavior. However, <c> dislocation loops generation and growth are caused by the net vacancy flux. These behaviors exactly follow the model structure. Dislocation loop discontinuities are caused by the limitation of the dislocation loop model [30] because the dislocation loop number density was based on the experimental result. It seems that there is a discrepancy of time scale of irradiation growth between the defect concentration/defect flux (shown in Fig. 3) and the number density of dislocation loop (shown in Fig. 4). However, that is misunderstanding originated from the difference of x-axis scale of each figure, i.e., the scale of x-axis in Fig. 3 is a logarithmic scale, while that in Fig. 4 is a standard one.

Finally, irradiation growth can be calculated using the defect concentration and sink density results. The results are compared with experimental measurements by Carpenter [11] in Fig. 5. Although the experimental values of the growth strain were higher than the calculation data at 2–6 dpa, the overall growth tendency is similar to that of the experimental database and other irradiation growth models [7,8]. The modeled result show a breakaway phenomenon, which is in good agreement with experimental data.

For single-crystal zirconium, dislocation loops have a stronger effect on irradiation growth than any other sink. Therefore, the results should be analyzed in terms of that factor, which determines the dislocation properties. Dislocation-induced irradiation growth depends on the defect flux, dislocation density, and bias factor. Among these three parameters, the dislocation density and bias factor are independent parameters. However, the defect flux depends on the function for the defect concentration that was calculated by the MFRT. The parameters in the MFRT are environment variables; hence, they should not be changed arbitrarily. In case of bias factor, it is derived from fundamental principles of physical chemistry. Therefore, it is hard to understand or derive in other research fields. Therefore, fundamental research has to be verified by a suitable professional. Therefore, the dislocation loop density is examined.

In this model of the dislocation density, the dislocation loop number density is the only independent parameter except for the

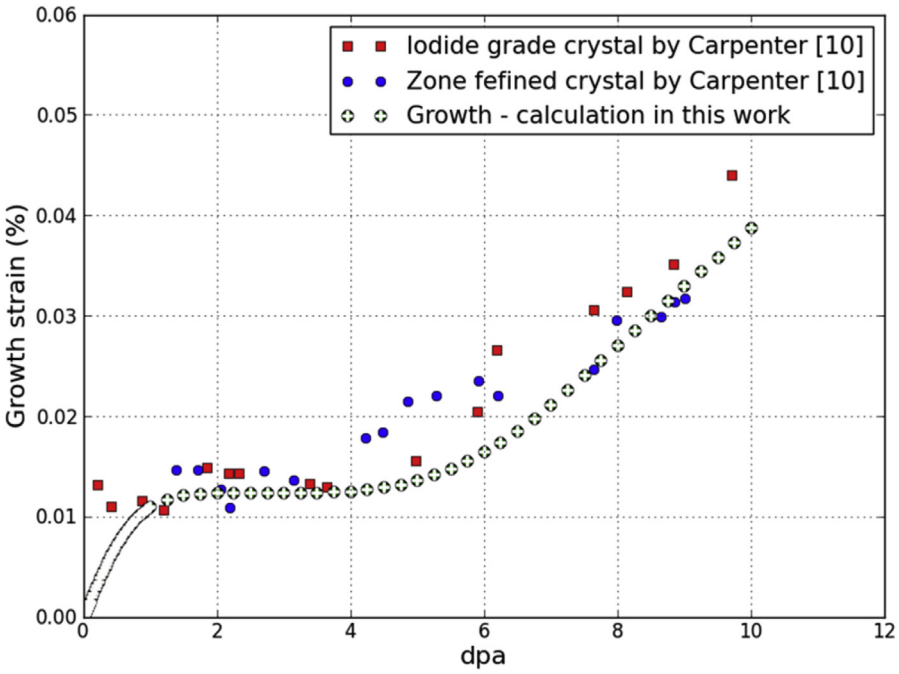

Fig. 5. Modeled and experimental irradiation growth strain in single-crystal zirconium at 553 K.

environment parameters such as the diffusivity, defect concentration, and Burgers vector. Therefore, the experimentally obtained number density of dislocation loops is used in this model [17,18]. Unfortunately, the only irradiation growth model that uses the number density of dislocation loop is the work of Barashev et al. [30]. Their modeling result was very similar to the calculated result in this paper. However, point defect clustering is currently used to calculate dislocation loops theoretically [8]. Therefore, the number density of dislocation loops should be verified using a theoretical method. However, in the work of Christien and Barbu, the number density of dislocation loops is not compared with experimental results.

3.2. Polycrystal zirconium

The results for a single crystal confirmed that a simplified model that does not include clusters matches the experimental result well. Except for the concept of the cluster, the dislocation density model used in this study is identical with that of Golubov et al. Therefore, it can be assumed that the cluster effect is negligible under this irradiation condition. Therefore, according to this assumption, irradiation growth of polycrystal zirconium is predicted. For annealed and cold-worked polycrystal zirconium, it was assumed that the diffusion coefficient was higher than that for single crystals because of enhanced grain boundary mobility. However, there is no general reference regarding enhanced grain boundary diffusion. Therefore, the diffusion coefficient effect was modified by the results of the cold-worked polycrystal zirconium code simulation. In cold-worked polycrystal zirconium, the modeled irradiation growth did not agree well with the experimental data. However, when the diffusion coefficient was modified by a factor of fifteen (15.0×10^{-6}), the irradiation growth result was in good agreement. Therefore, this diffusion coefficient was adopted for annealed polycrystals because annealed polycrystal zirconium also has the same grain boundary size.

3.2.1. Cold-worked polycrystal zirconium

In cold-worked polycrystal zirconium, the defect concentration shows typical high-sink-density behavior. As in single-crystal zirconium, the interstitial defect concentrations initially increase 10^{-11} up to 10^{-12} dpa. However, in cold-worked polycrystal zirconium, interstitial defect concentrations initially increase 10^{-10} up to 10^{-12} dpa. Next, the effect of the recombination rate can be neglected because of the high sink density. Therefore, the rate of decrease of the interstitial concentration is smaller than that in single-crystal zirconium. Finally, interstitial and vacancy concentrations are in a steady state. Fig. 6 (a) shows the defect concentrations in cold-worked polycrystal zirconium.

The net defect flux to the sinks are analyzed for <*a*> dislocation lines, <*c*> dislocation lines, and grain boundaries. Fig. 6 (b) shows the net defect fluxes to these sinks. The defect fluxes to sinks show quasi-steady-state regions instead of peaks, unlike the behavior in single-crystal zirconium. This phenomenon is caused by the high sink strength (the sink strength is sufficient to consume the defects at an early stage). Subsequently, as in single-crystal zirconium, the defect fluxes decrease. After 10^{-2} dpa, the net defect fluxes show a final steady-state region. Finally, these constant net defect fluxes determine the irradiation growth strain. Therefore, irradiation growth is accelerated by these constant fluxes to sinks.

Because the major sinks in cold-worked polycrystal zirconium are dislocation lines and grain boundaries, three types of sink are examined. Fig. 7 shows the dislocation line density and grain boundary sink strength versus the dpa. The dislocation line density was assumed to be a time-independent parameter. Therefore, the dislocation line density is constant with respect to the dpa. (Physically, the dislocation line density in cold-worked zirconium is already sufficiently developed. Therefore, it could not be increased because dislocation lines develop into network dislocations.) The grain boundary sink strength function depends on the dislocation line density. Therefore, the sink strength of grain boundaries also constant with respect to dpa.

Fig. 8 presents the model results for cold-worked polycrystal zirconium. The irradiation growth strain of cold-worked polycrystal

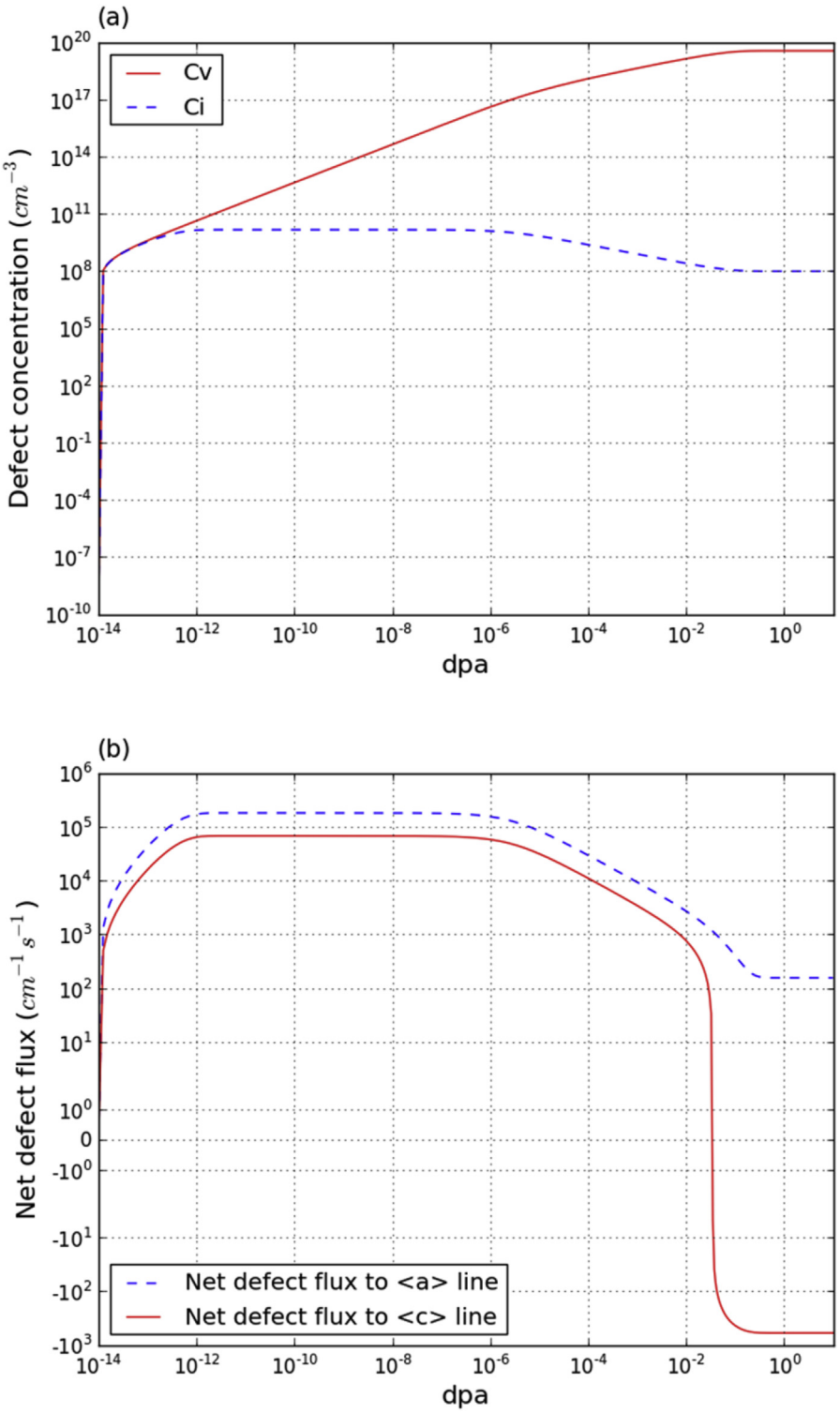

Fig. 6. Radiation induced (a) defect concentrations, and (b) net defect flux to dislocation line in cold-worked polycrystal zirconium at 553 K.

zirconium is also quite similar to experimental results [16]. In this case, dislocation line sink effects are dominant. Therefore, irradiation growth exhibits very simple behavior, i.e., a linear increase with dpa. The results for cold-worked polycrystal zirconium were compared to experimental data for cold-worked zircaloy because of an absence of cold-worked polycrystal zirconium reference data [35]. Fortuitously, most of the research has assumed that the effect of the alloy element in zircaloy is negligible because the dislocation line sink effects are so dominant [14,35].

In cold-worked polycrystal zirconium, dislocation lines are the most powerful factor in irradiation growth modeling. It was assumed that the dislocation line density is already saturated, so it is not increased by the defect flux. In dislocation-line-induced irradiation growth, the dislocation line density and defect flux

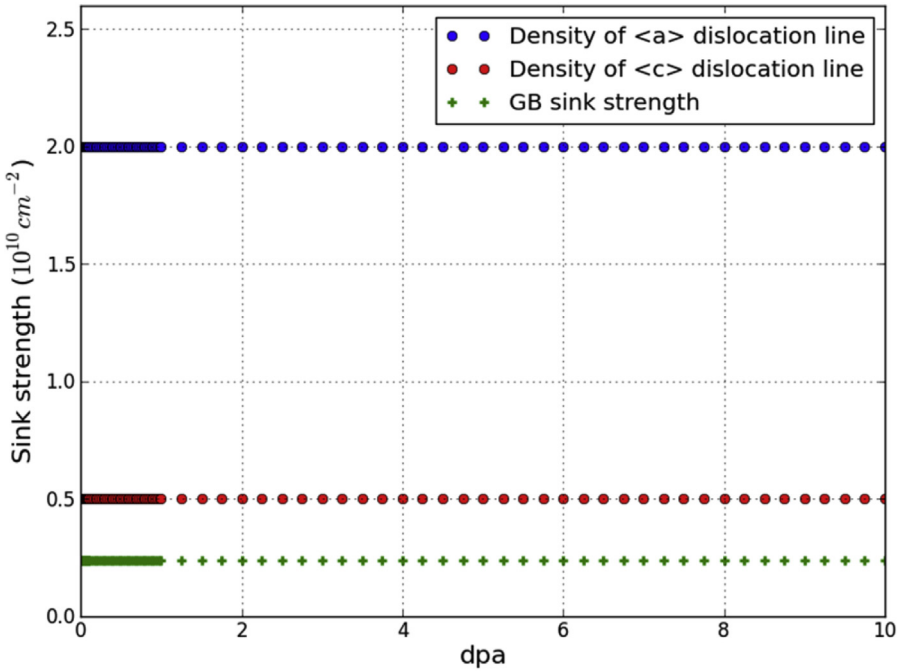

Fig. 7. Sink strength in cold-worked polycrystal zirconium at 553 K.

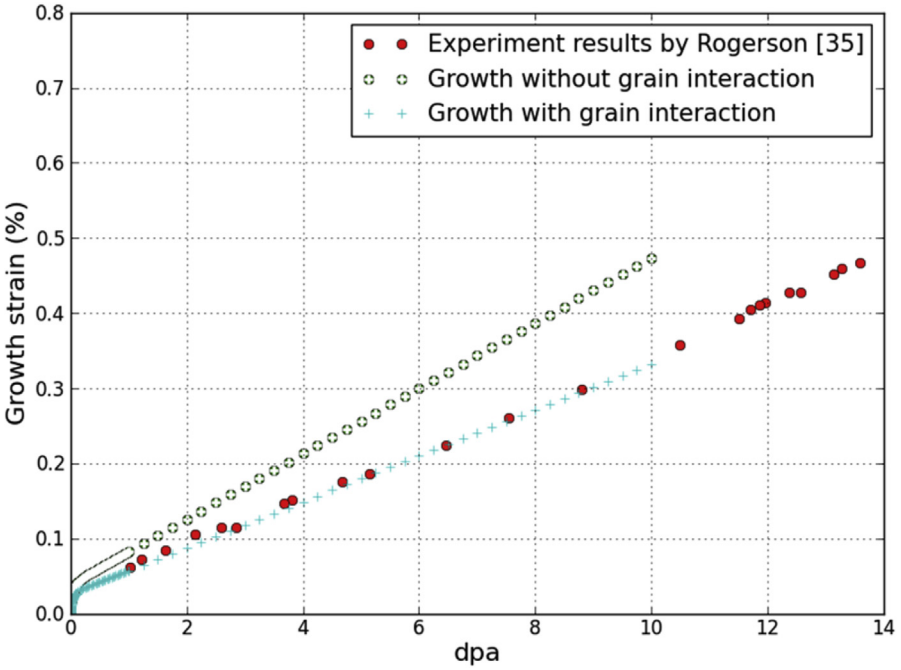

Fig. 8. Modeled and experimental irradiation growth strain in cold-worked polycrystal zirconium at 553 K.

and the bias factor determine the irradiation growth strain. Because it was assumed that the dislocation line density is constant, the bias factor is an independent parameter, as in single-crystal zirconium.

3.2.2. Annealed polycrystal zirconium

In annealed polycrystal zirconium, the defect concentration shows intermediate-sink-density behavior. As in the single-crystal and cold-worked cases, the defect concentration initially increases. Its subsequent behavior is similar to that in the cold-worked case. However, the quasi-steady-state region shows a much higher concentration because of the lower sink density. Fig. 9 (a) shows the defect concentration in annealed polycrystal zirconium.

For the behavior of the net defect fluxes to sinks, three types of defect are also analyzed because the major sinks are dislocation loops and grain boundaries. Fig. 9 (b) shows the net defect fluxes to sinks. As in cold-worked polycrystal zirconium, the sink strength is high enough to cause a steady state at low dpa (before 10^{-8}).

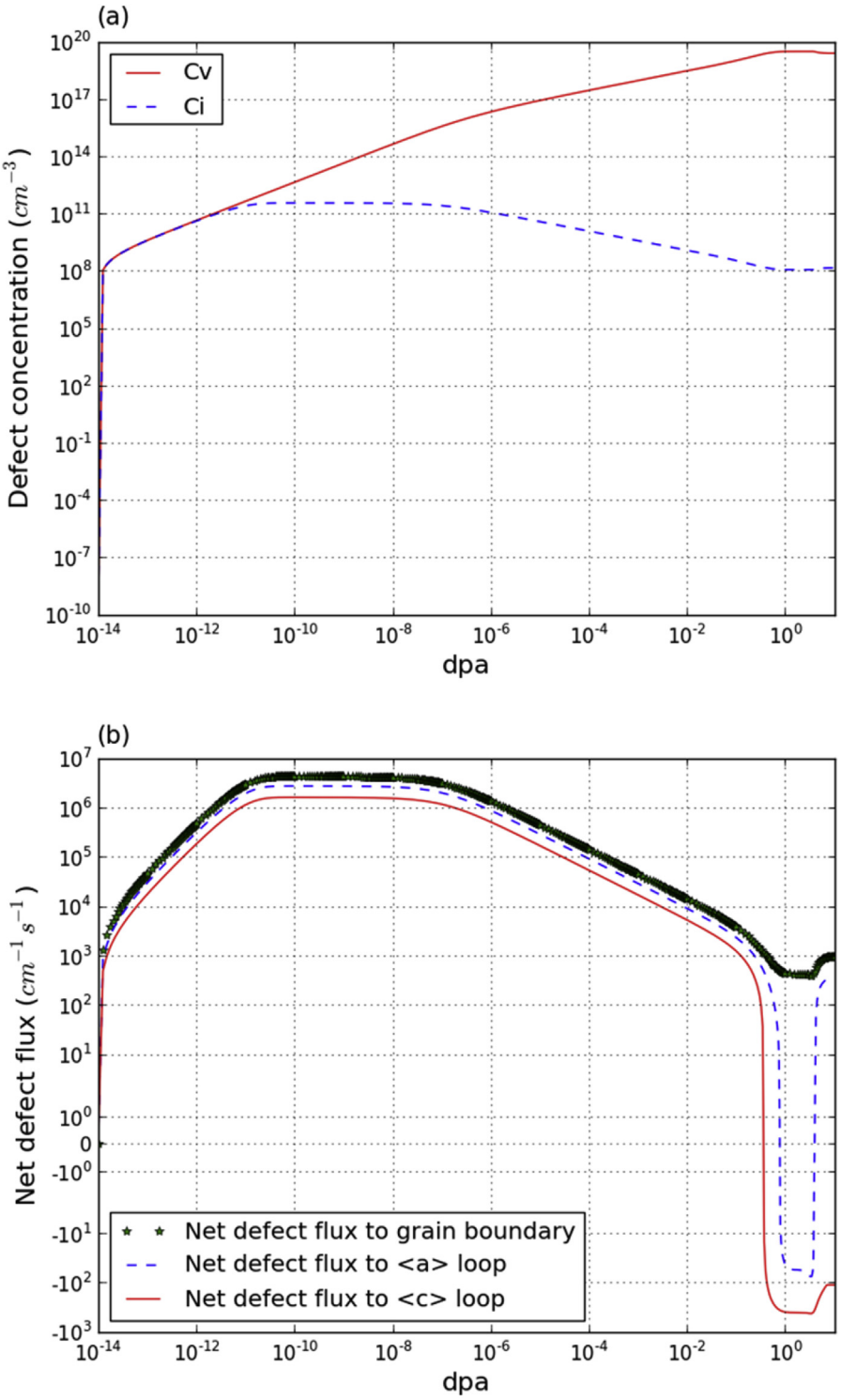

Fig. 9. Radiation induced (a) defect concentrations, and (b) net defect flux to dislocation loops and grain boundary in annealed polycrystal zirconium at 553 K.

However, the induced dislocation density in cold-worked polycrystal zirconium is much higher than that in annealed polycrystal zirconium. Therefore, the defect flux is much higher in annealed polycrystal zirconium than in cold-worked polycrystal zirconium.

In annealed polycrystal zirconium, the major sinks are <*a*> and <*c*> dislocation loops and grain boundaries. Therefore, these three types of sink are examined. Dislocation loop examined same method of single crystal. Fig. 10(a) shows the number density of dislocation loops. The value of the former is obtained from an experimental database [17,18], and the radius is calculated using the change rate of the total number of defects. Fig. 10(b) shows the dislocation loop radius. Unlike the case for the single crystal, the <*c*> dislocation loop radius is much larger than the <*a*> dislocation loop radius. Fig. 10(c) shows the dislocation loop density and grain boundary sink strength versus the dpa. The grain boundary sink strength increases with increasing dpa because it depends on the

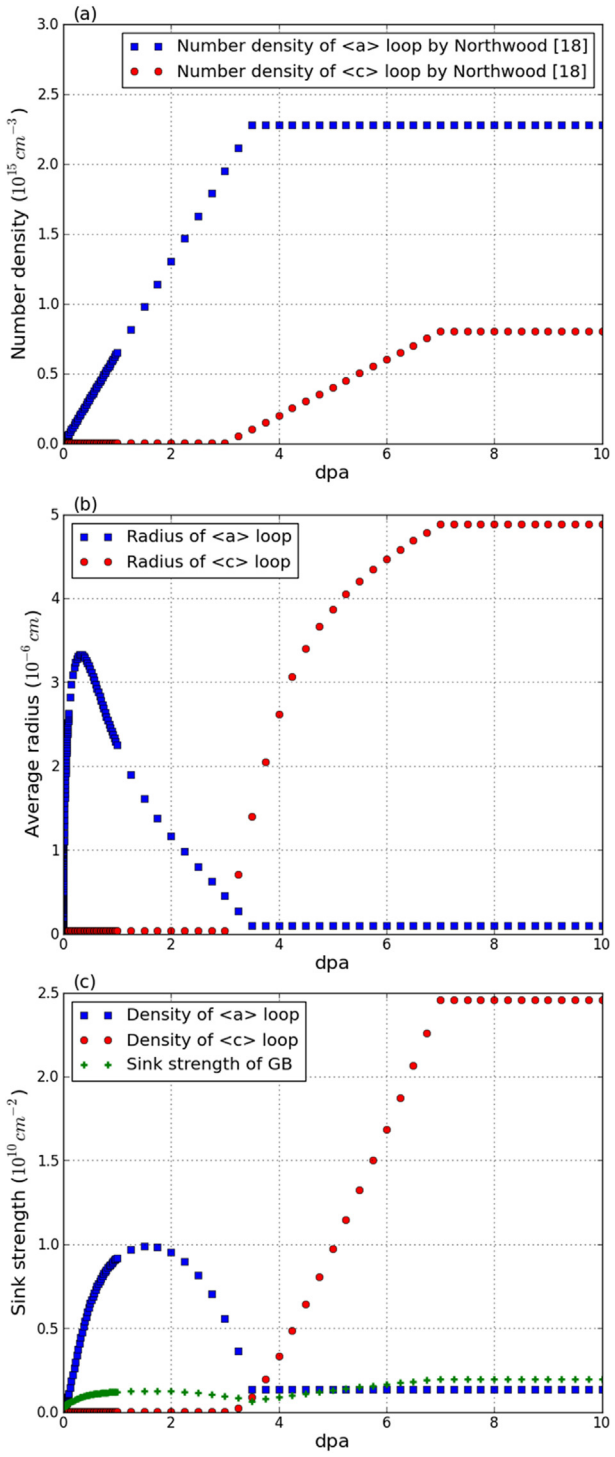

Fig. 10. Sink information of (a) number density, (b) average radius, and (c) sink strength in annealed polycrystal zirconium at 553 K.

dislocation line and loop density. The <*a*> dislocation loop density has the shape of a semicircle before 4 dpa, after which <*a*> dislocation loops are saturated. The increase in the <*c*> loop density resembles an exponential model. However, <*c*> dislocations have a much higher sink strength than <*a*> dislocation loops. This result does not match the experimental results well. Therefore, this advanced model clearly cannot be adopted for annealed polycrystal zirconium. Consequently, the assumptions for annealed polycrystal zirconium should be modified.

The strength model for grain boundaries is based on the dislocation line and loop densities. The dislocation lines are assumed to be constant with respect to the dpa. Therefore, the primary reason for the disagreement in the case of annealed polycrystal zirconium is dislocation loops. In this model, the sink strength of dislocation loops is calculated using experimental data on the number density. The behavior of the sink strength depends strongly on the number density. However, as in the case of a single crystal, there are no precise experimental data in the given dpa region. In the other cases, a new mechanism for the grain boundary strength should be suggested. However, there is currently no general theory or simulation result for the grain boundary sink strength.

The assumption about existence of the cluster might be the reason of the discrepancy in annealed polycrystal zirconium because the cluster was considered as dislocation loops in MFRT modeling. Recently many research activities on irradiation growth in zirconium and its alloy already have been done by using CDM. However, there is no guarantee that the accuracy of CDM is better than the old approach of using experimental sink densities and MFRT. In this work, calculation results for single-crystal and cold-worked polycrystal zirconium without considering the cluster is quite similar to the experiment result. From this result, it is difficult to determine that cluster is the reason for the disagreement in radiation growth of annealed polycrystal. Moreover, straight-forward master-equation-based formulation in CDM requires microscopic information on the particle-cluster reaction (forward and backward) for each cluster size, such as association and dissociation enthalpies and entropies of clusters, which is difficult to get and many empirical assumptions have to be made. Hence, to develop this method, various parametric information should be calculated and reaction probability by considering atomic configuration should be obtained [40,41]. Also, CDM is based on the diffusion-controlled kinetics to explain reaction between defect and cluster. Diffusion-controlled kinetics is not suitable method to predict the reaction between defect and cluster. In case of small clusters, reaction controlled kinetics is more suitable method to describe reaction probability. In this situation, MFRT is one of easy and simple tools to be applicable to and simulate various situation.

Stochastic fluctuations can be an alternative way to explain the deviate between calculation results and experimental database. In this approach, thermal and other noises could be taken into account in reaction probability. Because of complexity of CDM and PBM approach, classical rate theory based on stochastic fluctuation could be more suitable for anisotropic materials. However, in order to adopt this method, stochastic concept should be defined and understood in materials perspective. Hence this approach will be studied in the next step of the current study.

In this paper, the effect of residual stress on the anisotropy factor was neglected in annealed polycrystal. However, Causey et al. [23] revealed a profound effect of residual stress in irradiation growth. In specific case, irradiation growth occurs in opposite direction to relax the residual stress when it is present, and strain shows a common behavior after the relaxation. In order to comply with this effect, an upper-bound model can be used since the model used in this study is based on numerical method. Unfortunately there is no available data of residual stress of specimens of interest in this study. Moreover, the compliance of single crystal also should be calculated by Hill's criteria and Eshelby's model in hexagonal structural slip system. This method will be adopted in the next step of the current study.

If the general method of irradiation growth modeling is correct for annealed polycrystal zirconium, several parameters could also be the reason for this disagreement. First, the diffusion coefficient of grain boundaries could be the reason. It was calculated by many authors using their own computer simulation methods and

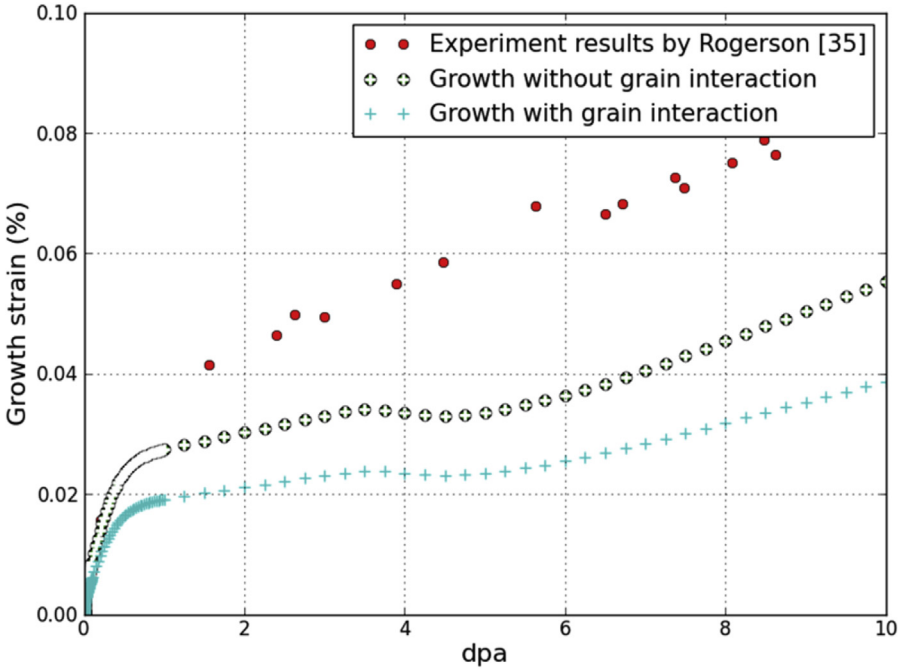

Fig. 11. Modeled and experimental irradiation growth strain in annealed polycrystal zirconium at 553 K.

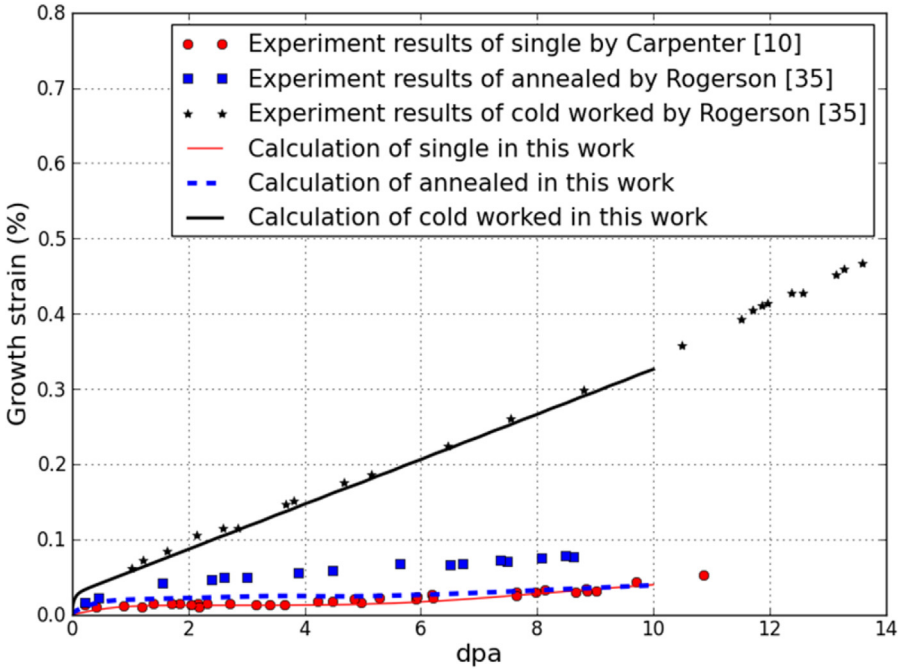

Fig. 12. Modeled and experimental irradiation growth strain in zirconiums at 553 K.

mechanisms [9,27]. Therefore, the results of these simulations differ from each other. The mechanism of diffusion at grain boundaries should be verified by fundamental research.

Fig. 11 shows the modeled growth in annealed polycrystal zirconium. Both results show high growth strain initially. However, after 1 dpa, the calculated strain shows a much slower increase. This difference between the calculation and measurement increases with increasing dpa. The sink strength data analysis confirmed that the behavior of the grain boundary sink strength and <*a*> and <*c*> dislocation loops are the source of this disagreement.

3.3. Path forward

In this study, irradiation growth of zirconium is calculated and analyzed using a simplified and generalized model of the MFRT. Fig. 12 show the result of irradiation growth of single-crystal and polycrystal zirconium. The calculation result agrees well with the

experimental result. However, in the nuclear industry, zirconium alloys such as zircaloy-2, zircaloy-4, and zirlo are widely used in cladding and structural material. Therefore, for precise analysis, defect information for these zirconium alloys should be suggested. Although the parameters used in this study are not those of zirconium alloy, the results could suggest fundamental concepts. Further, in cold-worked zirconium alloy, the effect of the alloy element could be negligible because the dislocation line sink strength is very strong. Therefore, the model and the calculation results in this study could provide a useful tool and a meaningful dataset for design and life prediction of zirconium components in nuclear reactors. In this study, however, several key parameters such as dislocation loop number density, diffusion coefficient, and defect generation rate were obtained from an experimental database of references. These limitations should be overcome in the next stage of research. The dislocation number density could be calculated using CDM modeling because each defect cluster is traceable in this model. Moreover, existence of vacancy dislocation loop in prism plane could be considered. The diffusion coefficient of zirconium could also be calculated by an advanced molecular dynamics simulation that includes an enhanced grain boundary diffusion coefficient. Finally, the defect generation rate will be considered to obtain precise irradiation growth modeling in the next research step. Therefore, fundamental research on atomic behavior using advanced tools could suggest a general irradiation growth model.

4. Conclusion

An irradiation growth model for single-crystal and polycrystal zirconium is established. The following summarizes the irradiation growth model in this paper. The defect concentration was calculated, and then the defect flux was derived using the diffusion coefficients for interstitials and vacancies in the MFRT. The growth strain equations were established for single-crystal zirconium and annealed and cold-worked polycrystal zirconium using the defect flux, bias factor, and sink strength. The results for single-crystal zirconium and cold-worked polycrystal zirconium are in good agreement with experimental results. An analysis of the behavior of the defect flux and sink strength demonstrated that the growth models are well established. However, for annealed polycrystal zirconium, the predicted irradiation growth deviates from experimental results because in this case, the sink behavior is more complex than in the single-crystal and cold-worked polycrystal cases. Therefore, for polycrystal zirconium, other parameters such as the diffusion coefficient and grain boundary sink strength should be analyzed at a more fundamental level.

Acknowledgement

This work was financially supported by the International Collaborative Energy Technology R&D Program (No. 20138530030010) of the Korea Institute of Energy Technology Evaluation and Planning (KETEP) funded by the Ministry of Trade Industry and Energy (MOTIE), and by the National R&D Program (No. 2011-0031771) through the National Research Foundation of Korea (NRF) funded by the Ministry of Science, ICT & Future Planning (MSIP).

References

[1] R.A. Holt, J. Nucl. Mater. 90 (1980) 193.
[2] S.R. MacEWEN, G.J.C. Carpenter, J. Nucl. Mater. 90 (1980) 108.
[3] A.J. Pedraza, D. Fainstein-Pedraza, J. Nucl. Mater. 88 (1980) 236.
[4] C.H. Woo, J. Nucl. Mater. 159 (1988) 237.
[5] C.H. Woo, J. Nucl. Mater. 276 (2000) 90.
[6] R.A. Holt, C.H. Woo, C.K. Chow, J. Nucl. Mater. 205 (1993) 293.
[7] S.I. Golubov, A.V. Barashev, R.R. Stoller, ONRL/TM-2011/473. (2011).
[8] F. Christien, A. Barbu, J. Nucl. Mater. 393 (2009) 153.
[9] Y.N. Osetsky, D.J. Bacon, N. De Diego, Metall. Mater. Trans. A 33 (2002) 777.
[10] G.J.C. Carpenter, R.A. Murgatroyd, A. Rorgerson, J.F. Watters, J. Nucl. Mater. 1981 (1981) 28.
[11] G.J.C. Carpenter, R.H. Zee, A. Rogerson, J. Nucl. Mater. 159 (1988) 86.
[12] R.A. Murgatroyd, A. Rogerson, J. Nucl. Mater. 79 (1979) 302.
[13] R.A. Holt, J. Nucl. Mater. 91 (1980) 311.
[14] A. Rogerson, J. Nucl. Mater. 154 (1988) 276.
[15] A. Rogerson, J. Nucl. Mater. 152 (1988) 220.
[16] A. Jostsons, R.G. Blake, J.G. Napier, P.M. Kelly, K. Farrell, J. Nucl. Mater. 68 (1977) 267.
[17] A. Jostsons, P.M. Kelly, R.G. Blake, J. Nucl. Mater. 66 (1977) 236.
[18] D.O. Northwood, At. Energy. Rev. 15 (1977) 547.
[19] D.O. Northwood, R.W. Gilbert, G.J.C. Carpenter, J. Nucl. Mater. 61 (1976) 13.
[20] S.I. Choi, J.H. Kim, Nucl. Eng. Technol. 45 (2013) 385.
[21] A.D. Brailsford, R. Bullough, J. Nucl. Mater. 69–70 (1978) 434.
[22] C.H. Woo, J. Nucl. Mater. 131 (1985) 105.
[23] A.R. Causey, C.H. Woo, R.A. Holt, J. Nucl. Mater. 159 (1988) 225.
[24] E.F. Ibrahim, J. Nucl. Mater. 159 (1981) 214.
[25] B.L. Adams, G.S. Clebinger, J.P. Hirth, J. Nucl. Mater. 90 (1980) 75.
[26] C.H. Woo, X. Liu, Philos. Mag. 87 (2007) 2355.
[27] R.C. Pasianot, A.M. Monti, J. Nucl. Mater. 264 (1999) 198.
[28] M. Kiritani, J. Nucl. Mater. 216 (1994) 220.
[29] R. Sizmann, J. Nucl. Mater. 69–70 (1978) 386.
[30] A.V. Barashev, S.I. Golubov, R.E. Stoller, ORNL/TM-2012/225 (2012).
[31] C.C. Dollins, J. Nucl. Mater. 59 (1976) 61.
[32] R.A. Holt, J. Nucl. Mater. 159 (1988) 310.
[33] R.A. Holt, In-Reactor Deformation of Zirconium Alloy omponents, ASTM STP 1505, in: B. Kammenzind, M. Limback (Eds.), Zirconium in the Nuclear Industry, American Society for Testing and Materials, 2009,, pp. 3–18. Zirconium in the Nuclear Industry ASTM STP 1505 (2009) 3.
[34] R.A. Holt, G.A. Bickel, N. Christodoulou, J. Nucl. Mater. 373 (2008) 130.
[35] A. Rogerson, J. Nucl. Mater. 159 (1988) 43.
[36] G.S. Was, Fundamental of Radiation Materials Science, Springer, 2007.
[37] A. Jostsons, P.M. Kelly, R.G. Blake, K. Farrell, Neutron Irradiation-Induced Defect Structures in Zirconium, ASTM STP 683, in: J.A. Sprague, D. Kramer (Eds.), Effects of Radiation on Structural Materials, American Society for Testing and Materials, 1979, pp. 46–61. Effects of radiation on structural materials ASTM STP 683 (1979) 46.
[38] R.A. Holt, R.W. Gilbert, J. Nucl. Mater. 116 (1983) 127.
[39] R.A. Holt, R.W. Gilbert, J. Nucl. Mater. 137 (1986) 185.
[40] E. Meslin, A. Barbu, L. Boulanger, B. Radiguet, P. Pareige, K. Arakawa, C.C. Fu, J. Nucl. Mater. 382 (2008) 190.
[41] A. Hardouin Duparc, C. Moingeon, N. Smetniansky-de-Grande, A. Barbu, J. Nucl. Mater. 302 (2002) 143.
[42] A. Rogerson, R.H. Zee, J. Nucl. Mater. 151 (1987) 81.
[43] M. Griffiths, J. Nucl. Mater. 159 (1988) 190.
[44] F. Onimus, J.L. Béchade, in: R.J.M. Konings (Ed.), Comprehensive Nuclear Materials, Elsevier, Oxford, 2012, p. 1.